ELSEVIER

Journal of Nuclear Materials 276 (2000) 202–212

journal of nuclear materials

www.elsevier.nl/locate/jnucmat

Interactions between mobile dislocation loops in Cu and α-Fe

Yu.N. Osetsky[a], A. Serra[b,*], V. Priego[b]

[a] *Department of Engineering, Materials Science and Engineering, The University of Liverpool, Brownlow Hill, Liverpool L69 3GH, UK*
[b] *Departament de Matemàtica Aplicada III, Universitat Politècnica de Catalunya, Jordi Girona 1-3 Mòdul C-2, 08034 Barcelona, Spain*

Abstract

The relevance of one-dimensionally gliding clusters in the understanding of the damage accumulation produced by the displacement cascades has been underlined by the production bias model. The properties and mobility of isolated clusters of vacancies and self-interstitials have been recently studied by molecular dynamics and valuable information about their diffusional characteristics is obtained. The next step in the understanding of radiation damage should include the possible reactions of these clusters with other clusters, dislocations and other sinks. In this paper we present the first results of a molecular dynamics study of interactions between glissile interstitial clusters and small dislocation loops in α-Fe and Cu. Different types of interactions have been studied between clusters of different sizes (from 12 to 91 defects) in the temperature range from 300 to 1000 K. As a result of the inter-cluster interactions both glissile and sessile clusters can be obtained and this depends on the metal, reaction type and size of the clusters. In general the probability to form sessile clusters increases for larger clusters and it is higher in Cu. The results obtained are discussed from the point of view of the difference in radiation damage effects in fcc Cu and bcc Fe.

1. Introduction

The significant success of the production bias model [1–3] in the description of radiation damage in Cu stressed the importance of the one-dimensionally mobile clusters of self-interstitial atoms (SIAs) in the creation of a large vacancy supersaturation at initial stages of irradiation [4,5]. This stimulated extensive studies of glissile clusters and dislocation loops and valuable information on the structure and properties of glissile SIA clusters and the mechanisms of their thermally-activated motion has been obtained during the two last years [6–14]. Very recently it was observed that stable perfect vacancy dislocation loops can also be mobile [9,15]. All recent studies of the glissile clusters considered isolated clusters and loops and aimed to establish the mechanisms of one-dimensional motion and the diffusion-like characteristics. On the other hand, the picture usually observed in the cascade region during simulation shows a variety of reactions between small clusters and other defects [16–18]. The reactions lead to different cluster transformations (sessile-to-glissile and vice versa), formation and growth of new clusters, change of glide direction of existing clusters, etc. Such reactions and interactions can be generalized for the bulk metal and should be an important input for modelling of damage accumulation and radiation hardening [19] in metals under cascade irradiation conditions.

In this paper we present the first results of molecular dynamics (MD) modelling of interactions between mobile clusters in Fe and Cu. The first aim of the study is to generalize the possible reactions between clusters in bcc and fcc lattices and to simulate some of them. The second aim is to find the qualitative differences in inter-cluster interactions between Fe and Cu which may contribute to our understanding of the difference in radiation damage accumulation in these two metals. Particular attention is paid to such reactions when a change in the properties of the interacting clusters and loops, e.g., Burgers vector or mobility, occurs.

* Corresponding author. Tel.: +34-93 401 6886; fax: +34-93 401 1825.
E-mail address: serra@etseccpb.upc.es (A. Serra)

0022-3115/00/$ - see front matter
PII: S0022-3115(99)00179-8

2. The relative orientation of interacting defects

In this section we underline the difficulties to define 'cluster' and 'dislocation loop' at an atomic level. Then we introduce the parameters needed to describe the relative position of the interacting defects since the final result of the interaction depends on it.

A considerable uncertainty exists in the definition of the difference between defect cluster and dislocation loop in atomistic simulation and this causes us to establish some agreement in using terms such as cluster and dislocation loop. It was found in previous studies that static and molecular dynamics simulations give different critical size for a cluster to become a dislocation loop. Thus, in static simulations of SIA clusters in Fe and Cu [10,20], a dislocation loop is defined qualitatively when the structure of the dislocation core can be clearly seen. For example, clusters in Fe having more than 16–19 SIAs have these features. Note that the Burgers vector can be identified even for smaller clusters by constructing the Burgers contour. MD simulations of SIA and vacancy clusters have shown that, at non-zero temperature, much bigger clusters can be described as sets of point defects but not dislocation loops [10,15]. Thus, a 91-SIAs cluster in Fe can be decomposed into individual crowdions during its thermally-activated movement over the wide temperature range from 240 to 860 K [12]. On the other hand such a cluster, having a diameter bigger than 2 nm, is visible in TEM as a small dislocation loop. Summarising this, we have to admit that up to now the set of properties that define a cluster and a dislocation loop is not well clarified. Therefore, in this paper we use terms cluster and 'loop' equivalently bearing in mind that the direction of the Burgers vector of a loop is equivalent to the glide direction of a cluster. In some simulations we have found different behaviour of clusters of different sizes and this is discussed in Section 5 from the point of view of possible difference between cluster and loop.

The analysis of the gliding process and properties of the most stable glissile clusters and loops (with Burgers vector $\frac{1}{2}\langle 1\,1\,1\rangle$ in α-Fe and $\frac{1}{2}\langle 1\,1\,0\rangle$ in Cu) shows that there are two main types of cluster–cluster and loop–loop interactions, e.g., when their Burgers vectors, or glide directions, are parallel, $\alpha = 0$, and when they are intersecting, $\alpha \neq 0$.

We have characterised the interaction between clusters by some parameters represented in Fig. 1. Two clusters of radii r_1 and r_2 that move along the lines defined by their Burgers vectors have been considered.

The simplest case shown in Fig. 1a appears when the loops Burgers vectors are parallel, e.g., $\alpha = 0$ (type 1). The parameter D_C characterises the distance between the centres of mass (CMs) of loops. If loops are not overlapping $D_C \geqslant d_C = r_1 + r_2$, whereas if loops overlap $D_C < d_C$. The other parameter characterising this case is the distance between habit planes of the loops, ΔZ.

To characterise the interactions of type 2 depicted in Fig. 1b, i.e., between loops with non-parallel Burgers vectors ($\alpha \neq 0$), we introduce the parameter L_C equal to the minimum distance between the trajectory lines of the CM of loops (criss-crossed trajectories). In the limiting case, $L_C = 0$, the trajectories of the CM intersect. If $L_C \geqslant d_C$ the clusters do not overlap while if $L_C < d_C$ the

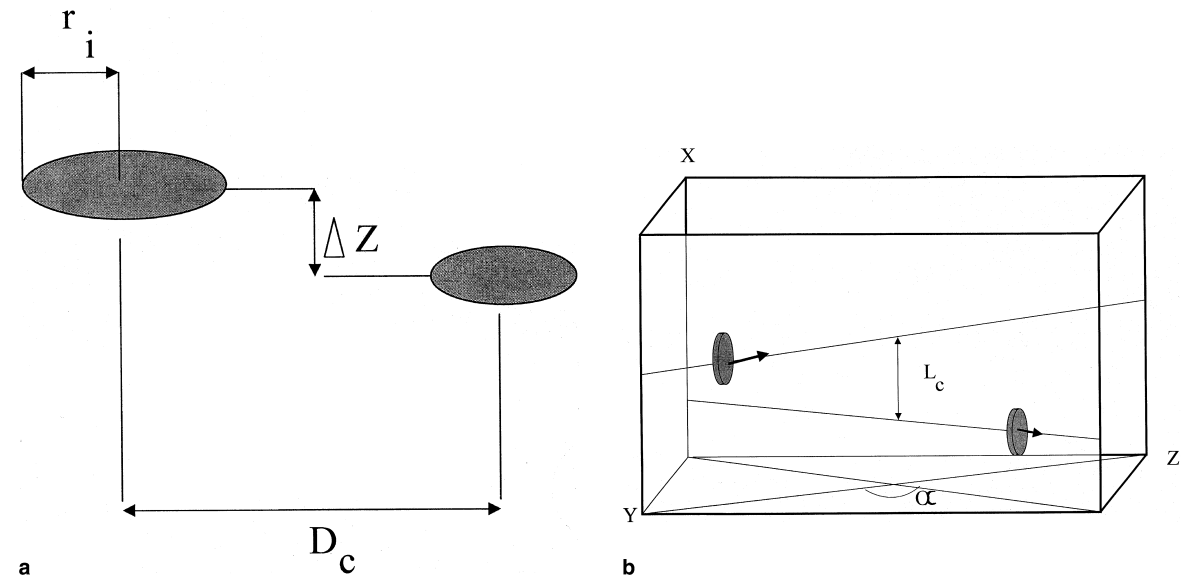

Fig. 1. Scheme of the simulated system with the parameters described in Section 2: (a) clusters with parallel Burgers vector; (b) clusters with criss-crossed trajectories.

deformations of the lattice created by each cluster along their crowdion direction overlap. The initial configuration can be characterised by the distance from the loop centre to the meeting point L_1, which can be different for each loop.

The geometry of type 1 interactions is qualitatively the same in bcc and fcc lattices whereas that of the type 2 can be different. The difference arises from the different angles between the $\langle 1\,1\,1\rangle$ vectors in the bcc lattice and the $\langle 1\,1\,0\rangle$ vectors in the fcc one. Thus, in bcc the angle between all $\langle 1\,1\,1\rangle$ directions is $\alpha = 70.5°$. Taking any two intersecting $\langle 1\,1\,1\rangle$ directions, it can be seen that a loop can approach the other one from two opposite sides and therefore we should consider two angles – acute, $\alpha = 70.5°$ and obtuse, $\alpha = 109.5°$. In the fcc lattice there are two possible angles between $\langle 1\,1\,0\rangle$ directions, namely $\alpha_1 = 60°$ and $\alpha_2 = 90°$. Taking into account the above consideration of acute and obtuse angles for the approaching loops, three possible angles $\alpha = 60°$, 120° and 90° should be considered here.

3. Computational model

The interactions were studied in rectangular crystallites containing two or more clusters. Special attention should be paid to the boundary conditions applied in a dynamic simulation of the interactions between extended defects. Since the displacements along the crowdion direction could be extended to few tens of lattice parameters [12,15,21], the widely used fixed boundary conditions cannot be applied in such studies because of the interactions between clusters and boundaries. The simulation of a SIA cluster in a crystallite with the size along the crowdion direction smaller than the corresponding range of deformations would result in an interaction with the boundaries forcing the cluster to be preferentially in the centre of the simulated crystallite. In the case of periodic boundary conditions, the main problem is related to the interactions of one cluster with the images of the other cluster. Thus, these simulations require big simulated crystallites, which makes each simulation rather difficult and time consuming. In the present study we used periodic boundary conditions for crystallites containing from 90 000 to 170 000 mobile atoms.

The crystallites were oriented in such a way that, if $\alpha \neq 0°$, the plane formed by the Burgers vectors of the clusters coincides with a plane $z =$ constant and, if $\alpha = 0°$, the clusters themselves are located in planes $z =$ constant. This allows to create systems that are easier to analyse and have an optimised number of atoms. Thus, for Fe, the X, Y and Z axes were along the directions [1 0 0], [0 1 1] and [0 $\bar{1}$ 1] for $\alpha \neq 0°$ and [1 $\bar{1}$ 0], [1 1 $\bar{2}$] and [1 1 1] for $\alpha = 0°$, whereas for Cu the axes were along the directions [1 $\bar{1}$ 0], [1 1 $\bar{2}$] and [111] for $\alpha \neq 0°$ and [1 0 0], [0 1 1] and [0 $\bar{1}$ 1] when $\alpha = 0°$.

In each simulation the clusters were first relaxed by a static method. After this relaxation the crystallite was heated to a particular temperature and molecular dynamics was used to model their evolution. During dynamic simulation the configuration of

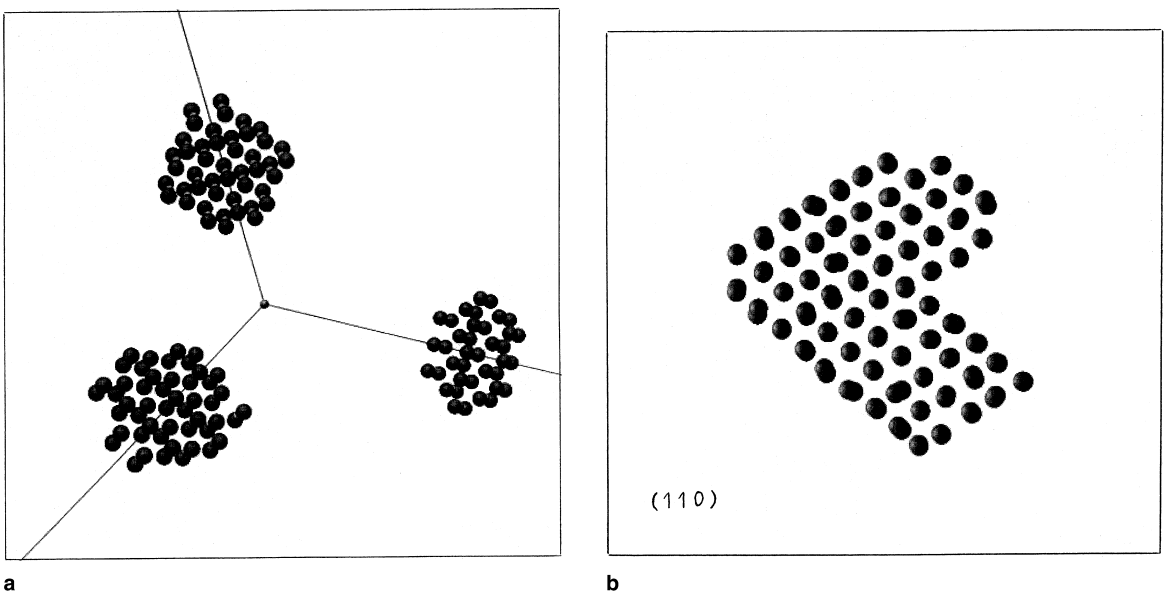

Fig. 2. (a) Projection of three Cu clusters on the (1 1 $\bar{1}$). Each interstitial is represented by two atoms (big spheres) and a vacancy (small sphere located in the perfect lattice site). (b) Glissile cluster projected along the crowdion direction [1 1 0] resulting from the attraction and reorientation of the three clusters shown in (a).

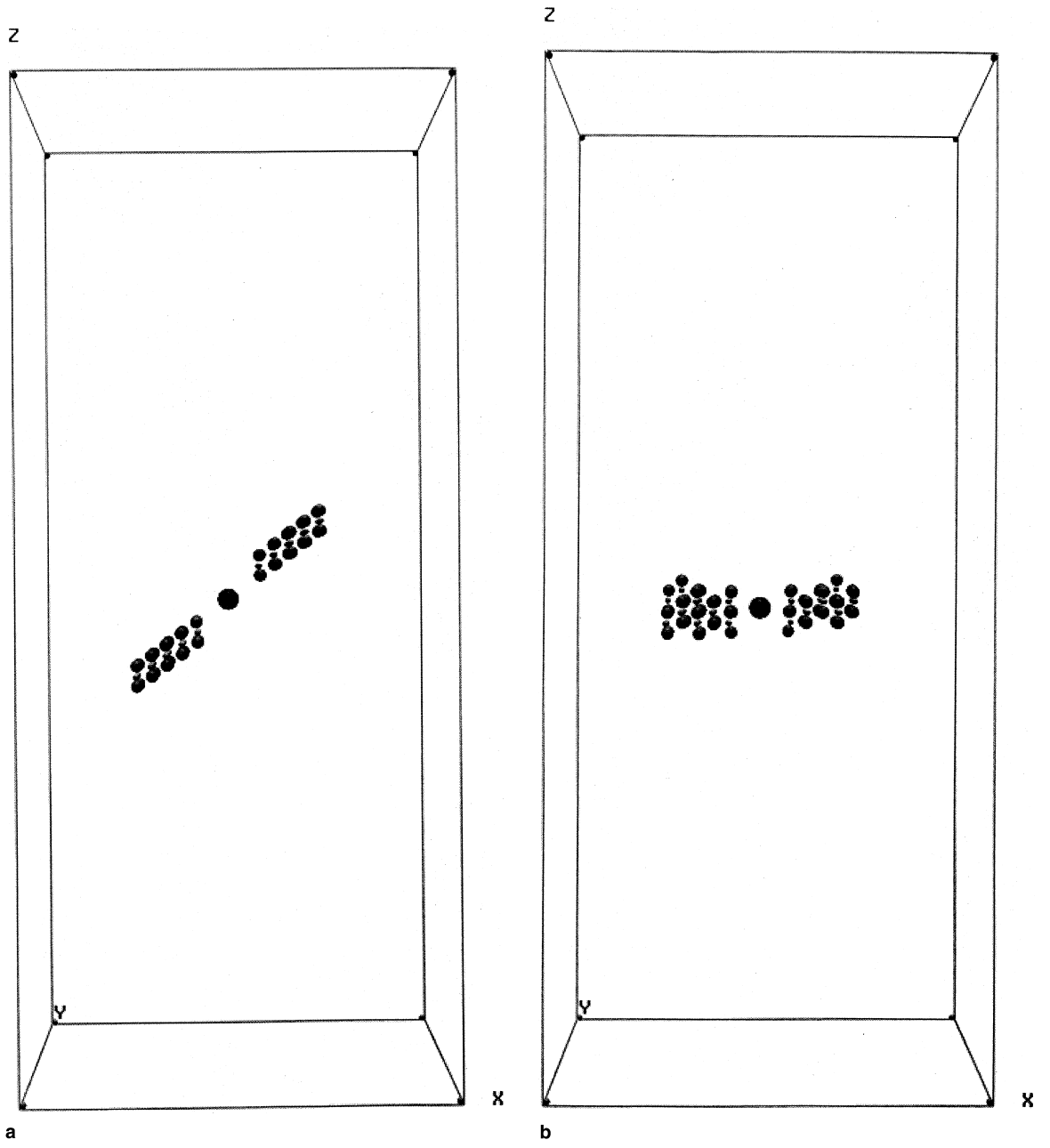

Fig. 3. (a) Two Cu clusters of parallel Burgers vectors initially at $\Delta Z = 3.5a$ after a static relaxation and (b) same clusters after 3 ps of dynamic simulation. The big sphere in between shows the position of the common centre of mass. The limits of the simulated box are indicated by the solid lines.

clusters was monitored using the trajectory viewer code ATOMTV. The details of cluster analysis can be found in [10].

For both metals we used the long-range pair interatomic potentials obtained in Ref. [22] and widely used earlier in the simulation of vacancy and interstitial clusters [7,9–12,15,23,24].

4. Results

Our study has shown that the final state of the interaction is dependent on the initial orientation of clusters and therefore in the following we describe separately all the cases studied showing in the headings of sections the values of the parameters characterising the

relative orientation together with the temperature simulated.

4.1. Interactions in Cu

4.1.1. $\alpha = 60°,\ L_C = 0,\ T = 800\ K$

Three loops of 19, 23 and 25 SIAs with Burgers vectors [1 0 1], [0 1 1] and [1 $\bar{1}$ 0] were located in such a way that the trajectories of their CM intersect in the centre of the crystallite (Fig. 2(a)). Initially the clusters were located in the vertexes of a triangle of sides 9*a*, 9*a* and 6*a*, where *a* is the lattice parameter. After few ps of simulation the two nearest clusters (of 23 and 25 SIAs), initially separated by about 6*a*, *attracted* each other and one of them had *reoriented* its crowdions one-by-one forming a glissile cluster of parallelepiped shape of 48 SIAs. The third cluster (of 19 SIAs) after 3–4 ps repeated the same sequence of events, i.e., approached the new cluster and then reoriented its crowdions one-by-one. The final cluster of 67 SIAs was mobile with the shape shown in Fig. 2(b).

4.1.2. $\alpha = 60°,\ L_C = d_C,\ T = 800\ K$

Two clusters of 24 and 10 SIAs were initially located at a distance $L_I \approx 9a$ to the meeting point. Their trajectory lines were separated a distance $L_C = d_C$ and, therefore, the clusters did not overlap. The clusters have approached very fast until they were separated by a distance of 3–4*a* and then they spent some time moving forward and backward keeping the distance between the CMs. Then they joined forming a three-dimensional complex with an immobile CM. Finally, after 10 ps, the crowdions of the smaller cluster reoriented parallel to the big one, i.e., the small cluster changes its Burgers vector, and a 34 SIAs glissile and mobile cluster was formed.

4.1.3. $\alpha = 90°,\ L_C = 0,\ T = 800\ K$

Two clusters with $N_I = 23$ were located at the same distance L_I to the point of intersection of their trajectories. The clusters have quickly (2–3 ps) approached and they kept their initial orientations. As a result a three-dimensional complex is formed where the two clusters make small oscillations but its CM is immobile during 20 ps. We notice here that both clusters kept their initial characteristics, e.g., shape and Burgers vector.

4.1.4. $\alpha = 0°,\ L_C = 2d_C,\ T = 310,\ 800\ K$

For this type of interaction it was found that the final configuration depends on the initial relative position of clusters (ΔZ) and temperature. We studied two clusters with $N_I = 19$ separated with $L_C = 2d_C = 4a$ for different separations between habit planes ΔZ.

If the initial separation is small, for example $\Delta Z = 3.5a$, the clusters attract each other and after the static relaxation it can be clearly seen how they are bent due to the attractive forces between them (see Fig. 3(a)).

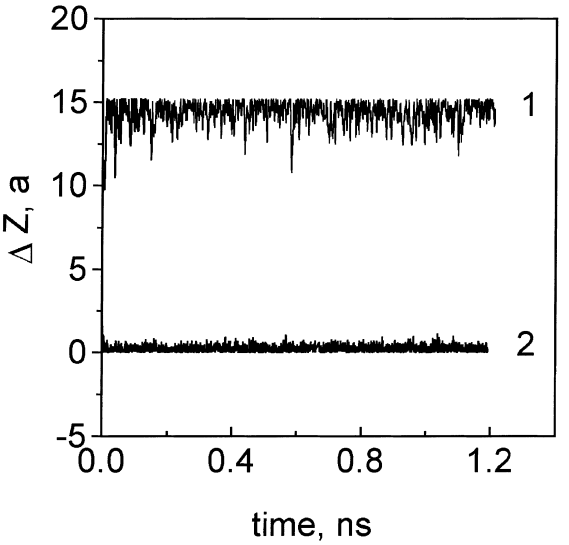

Fig. 4. Temporal evolution of the distance between the habit planes of two 19-SIAs clusters in Cu with parallel Burgers vectors simulated at 310 K for different initial separation (1) $\Delta Z = 9.5a$ and (2) $\Delta Z = 3.5a$.

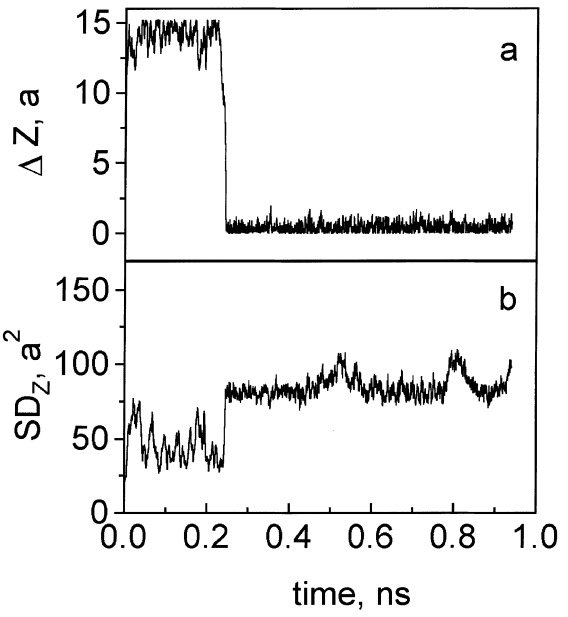

Fig. 5. Results obtained in the simulation of two 19-SIAs clusters in Cu with parallel Burgers vectors during annealing at 830 K initially separated with $\Delta Z = 9.5a$: (a) distance between the loops habit planes and (b) sum of the square of atomic displacements projected onto the glide direction.

In dynamic simulation clusters quickly (2–3 ps) were positioned in the same plane as shown in Fig. 3(b). Further simulation has shown (see Fig. 4 curve 2) that the oscillation of their CMs is rather small (maximum $\pm 0.5a$). We have estimated the characteristics of mobility of both clusters and their common centre of mass. It was found that the jump frequency of both clusters is about $\nu_{19} = 0.11 \times 10^{12}$ s^{-1} whereas that of their CM $\nu_{CM} = 0.065 \times 10^{12}$ s^{-1} which is about 4–6 times lower than the jump frequency obtained for individual clusters in Cu [10,11]. However the most significant changes occur with the correlation factor which was found to be less than unity, i.e., about 0.52 for individual clusters and 0.82 for their CM (for details of the calculation of the correlation factor see [10–12]). Similar behaviour has been observed for both temperatures. All this means that the mobility of such complex decreases very much and it does not produce significant displacements in the crystallite. (This can be clearly seen in Fig. 10 curve 2 in Section 5 where squared displacements in Fe and Cu are compared.) In other words, such interaction suppresses mobility of clusters.

If initially the clusters are separated by a large enough distance, for example $\Delta Z = 9.5a$, the result of the interaction depends on the temperature. Thus, at low temperature (310 K) they repulse each other. Due to the periodic boundary conditions their final position cannot be separated more than half of the crystallite size in the direction of $\vec{b}$. In the studied crystallite this distance was $\Delta Z_{MAX} = 15a$. Further simulation had shown that this configuration is rather stable and we could observe only oscillations near the maximum separation. It can be seen in Fig. 4 curve 1 that the amplitude of these oscillations is rather large (up to $\approx 4 - 5a$) which means that the repulsive interaction is rather weak, at least in comparison with the attractive interaction when the two clusters are in the same plane (see above). At high temperature (830 K) the repulsion can be overcome and clusters can join each other. This can be seen in Fig. 5(a) where clusters initially went apart but after about 250 ps they join each other. Further evolution is similar to the previous case when the initial separation is small. It is interesting to note that joined clusters are practically immobile and do not produce displacement of atoms in the crystallite. This can be seen in Fig. 5(b) where the temporal evolution of the projection of squared displacements of atoms onto the glide direction is presented.

4.2. Interactions in Fe

4.2.1. $\alpha = 109.5°$

Fig. 6(a) shows two clusters of 61 and 37 SIAs with $L_C = d_C$. They were annealed at $T = 1000$ K. Initially they approached very fast and formed the complex shown in Fig. 6(b). During about 60 ps it was no reorientation of crowdions and the complex shown in the figure was immobile. Then, the mechanism of reorientation of crowdions operated resulting in a glissile 98 SIAs cluster with the orientation of the former 61 SIAs cluster, as shown in Fig. 6(c).

Two clusters of $N_I = 19$ with $L_C = \frac{1}{2} d_C$ and centres separated a distance of about $9a$ were annealed at $T = 800$ K. They showed a weak interaction and approach slowly. Only after more than 20 ps the clusters have approached and after 9 ps the crowdions of one of them were reoriented and they have formed a single mobile cluster of $N_I = 38$.

For the case $L_C = d_C$ the same clusters of 61 and 37 SIAs shown an interaction of strongly repulsive character when they were annealed at $T = 1000$ K.

Vacancy–interstitial loop interaction. Since perfect vacancy loops in Fe can also be mobile [15] we tested the interaction between gliding vacancy and interstitial loops. We have simulated two loops of the same size, both containing 61 defects in the obtuse configuration ($\alpha = 109.5°$) with $L_C = 0$ at $T = 800$ K. The interaction was found to be very strong and both loops quickly moved towards the meeting point. The result of the interaction was a perfect crystal because all vacancies and interstitials were annihilated.

4.2.2. $\alpha = 70.5°$

When the angle is acute, the clusters joined each other and, depending on the size and temperature, the smaller cluster could change $\vec{b}$ and completely join the bigger one. We have studied the interaction between clusters and loops of different sizes from 19 to 61 SIA and only in the case of the two biggest loops (each has 61 SIAs) we have not observed re-orientation after a simulation of 120 ps.

During the process of crowdions reorientation we have observed that part of the interstitials changed to $\langle 1\,0\,0 \rangle$ crowdions that formed a squared cluster. However, in the studied cases, when clusters of 19 and 37 SIAs were reoriented, the size of $\langle 1\,0\,0 \rangle$ nuclei were too small to be stable at $T = 800$ K and finally all the interstitials were re-oriented again as $\langle 1\,1\,1 \rangle$ crowdions. This mechanism can contribute to the formation of $\langle 1\,0\,0 \rangle$ loops in Fe which have been observed experimentally at high temperature and discussed widely in [25,26].

4.2.3. $\alpha = 0°$

The interactions between clusters with parallel $\vec{b}$ have been studied in detail. We have simulated the interaction of a big loop $N_I = 91$ with small clusters $N_I = 19$ for different distances e.g., $L_C > d_C$, $L_C < d_C$ and $L_C = d_C$ at $T = 600$ and 1000 K. In all the simulations the initial configuration was formed by a loop of $N_I = 91$ in the centre of the system and three clusters located in planes above and below the big loop.

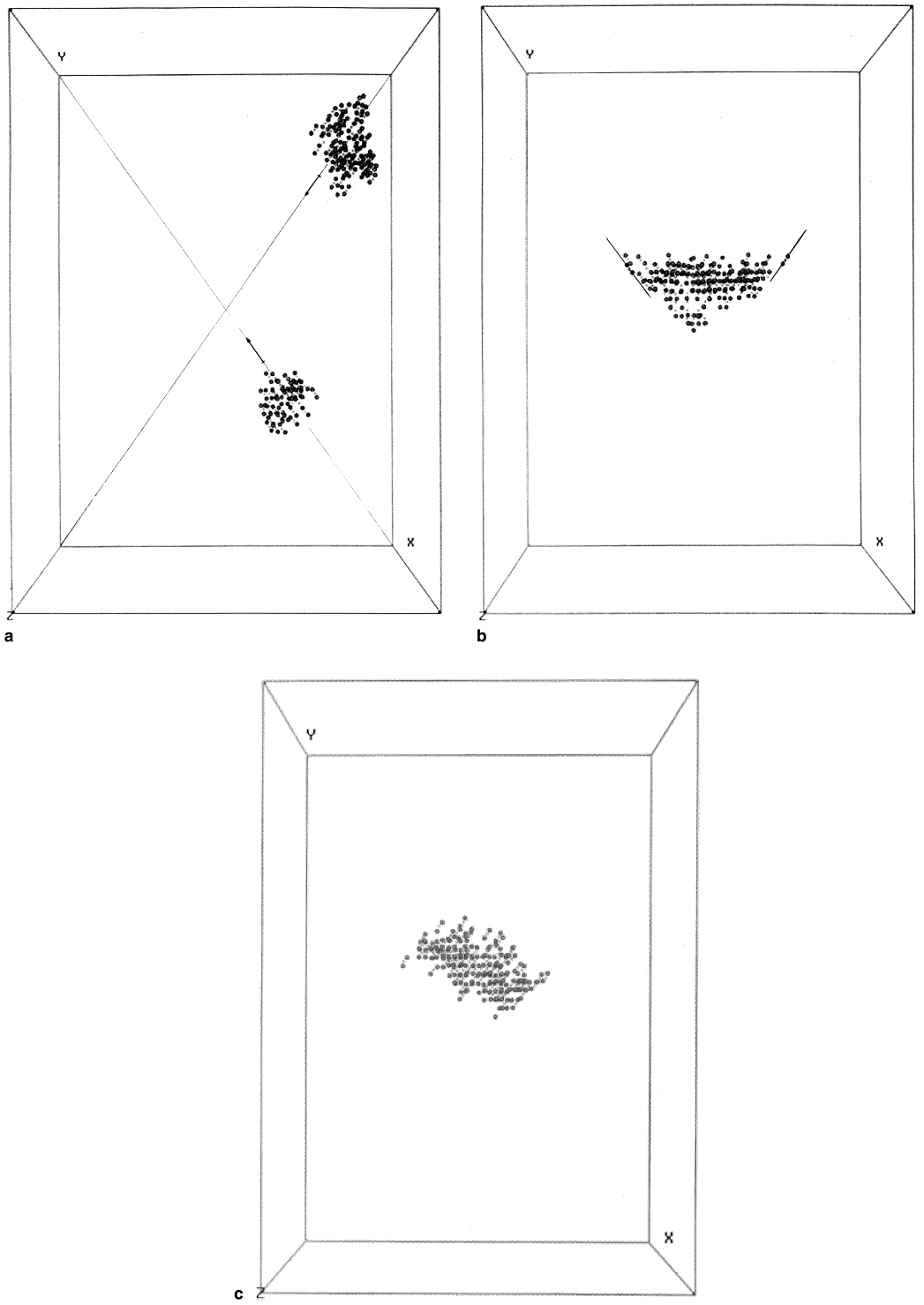

Fig. 6. (a) View along the [1 1 0] direction of two Fe clusters of 61 and 37 SIAs with relative orientation of $\alpha = 109.5°$ and $L_C = 0$. The arrows show the respective Burgers vectors of the $\langle 1\,1\,1 \rangle$ type. (b) Complex formed during the annealing at $T = 1000$ K of the configuration presented in (a). Note that the crowdions of the right cluster have different orientation that the ones of the left. (c) Cluster of 98 SIAs formed by the re-orientation of the 37 SIAs cluster.

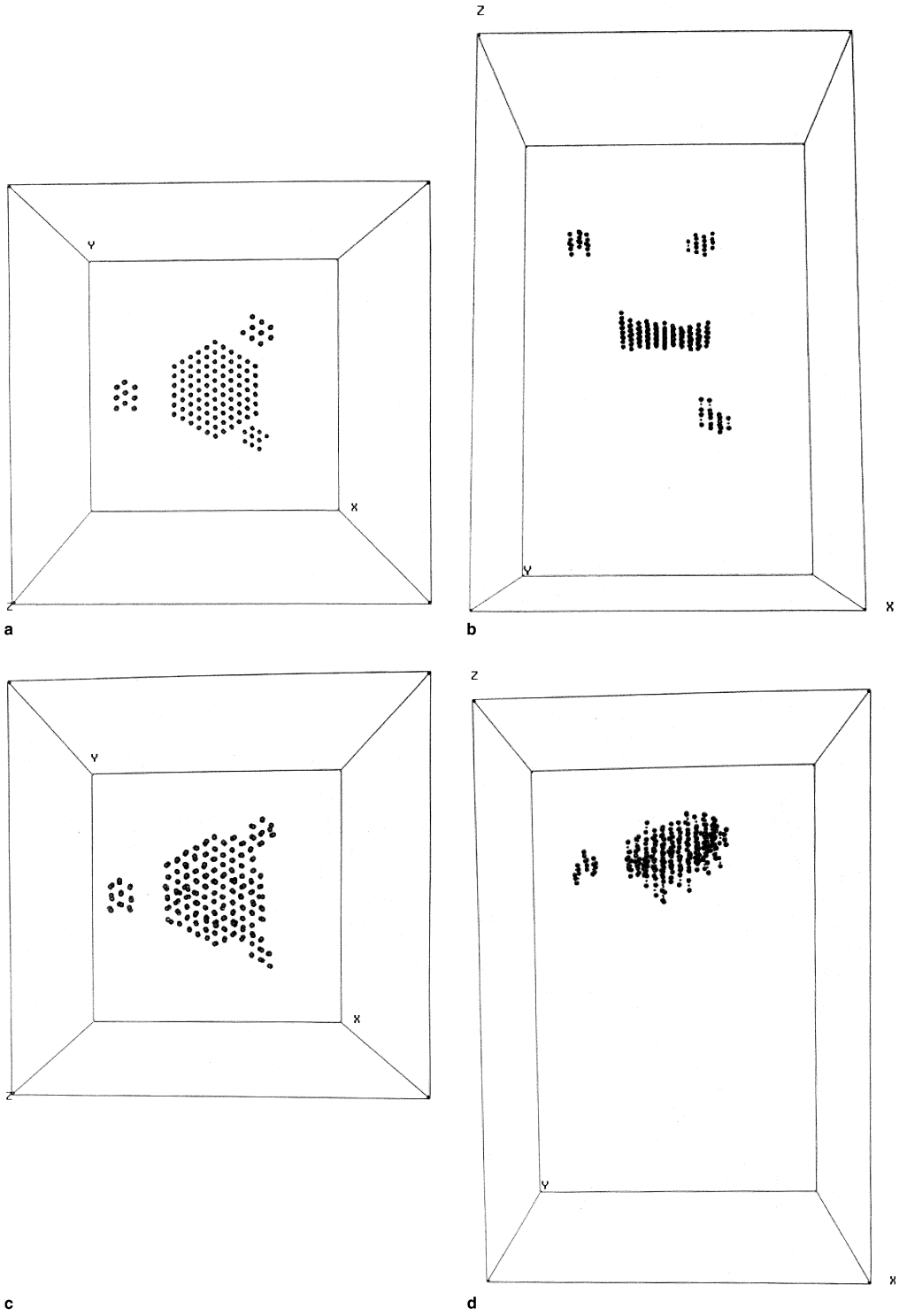

Fig. 7. 91 SIA loop together with three clusters of 9 interstitials in Fe. (a) and (b) show two views, along the crowdion direction and perpendicular to it respectively, of the statically relaxed complex before the dynamic relaxation. (c) and (d) show the same views after 220 ps of annealing at $T = 1000$ K. It can be seen that the clusters in the right have undergone a conservative climb to join the loop.

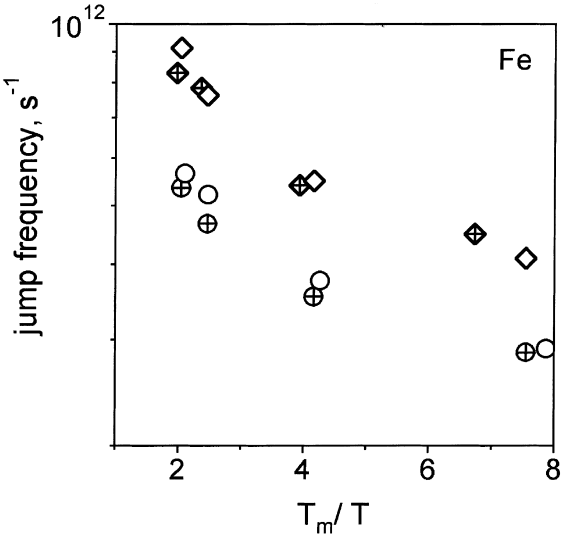

Fig. 8. Jump frequency versus reciprocal temperature obtained for different clusters in Fe: open diamond – isolated 19-SIA cluster; crossed diamond – averaged for two interacting 19-SIA cluster; open circle – isolated 37-SIA cluster; crossed circle – centre of mass of two 19-SIA clusters.

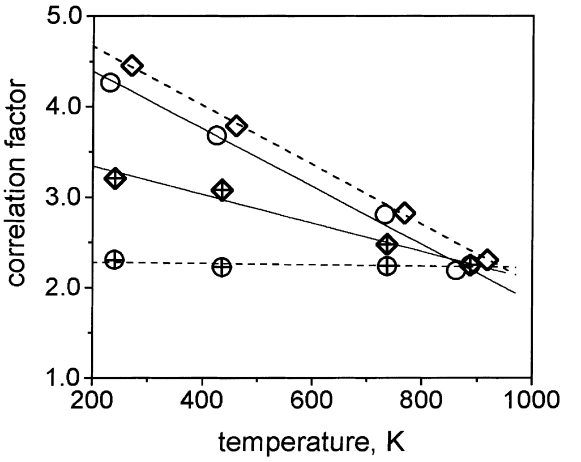

Fig. 9. Temperature dependence of correlation factor: open diamond – isolated 19-SIAs cluster; crossed diamond – averaged for each interacting 19-SIAs cluster; open circle – isolated 37-SIAs cluster; crossed circle – centre of mass of two 19-SIAs clusters.

$L_C < d_C$. When clusters are overlapping the interaction depends on how much they overlap. For a small overlap (one layer of interstitials) the smaller cluster joined the bigger one demonstrating the climb aside and thus forming a single glissile cluster. If the overlapping is bigger the smaller cluster has been repulsed.

If $L_C = d_C$ attraction is very strong and the small cluster joins the big one very quickly and for small $\Delta Z < 10$–$15a$ it can happen even athermally during the static relaxation. This interaction results with a single glissile cluster of irregular shape which can change by further diffusion of individual interstitials along the edge of the cluster.

$L_C > d_C$. Fig. 7(a) shows a view along the crowdion direction of a 91 SIA loop with three 19 SIAs clusters. The two clusters represented by bigger symbols are above the loop, the separation distances cluster-loop in the projection plane are $\sqrt{2}a$ and $2\sqrt{2}a$, respectively, where a is the lattice parameter. The other cluster represented by smaller symbols is below the loop and it is separated by $\sqrt{2}a$. Fig. 7(b) shows a view along a $\langle 1\,1\,0\rangle$ direction of the same system after a static relaxation. The small clusters are attracted by the big loop and create a glissile complex. Fig. 7(c) shows that, if the distance between the edges of clusters is small ($L_C = d_C + \sqrt{2}a$), the small clusters can be completely absorbed by the big one by a process of conservative climb. However, if the distance is bigger ($L_C \geqslant d_C + 2\sqrt{2}a$) the probability of conservative climb decreases drastically. Fig. 7(c) and (d) shows the system after 220 ps of dynamic simulation at $T = 1000$ K.

A detailed study was made with two clusters of 19 SIAs separated with $L_C = 2d_C$ and we have obtained dynamic characteristics such as the jump frequencies of the CM of each cluster and their common CM. The results are presented in Fig. 8 together with the results obtained for individual compact clusters of 19 and 37 SIAs. The analysis has shown that the jump frequency of each 19 SIAs cluster is the same as for the individual cluster of the same size and shape. The jump frequency of the common CM is just slightly smaller than that of the 37 SIAs cluster and in general we can accept that the mobility of such complex is close to the mobility of a compact cluster with the same amount of crowdions. However, the correlation factors of the individual clusters and their common CM have changed significantly as it is shown in Fig. 9. The value of the correlation factor of both 19 SIAs clusters decreases especially at low temperature. The value of the correlation factor of CM of two clusters also decreases and becomes almost temperature-independent.

5. Remarks and conclusions

Glissile clusters are formed by sets of crowdions that introduce a strong asymmetric deformation along the crowdion direction. Consequently, the interaction between clusters depends on their relative orientation. In this work we have classified the interactions according to the angle formed by the Burgers vectors of the clusters (α) and the position of their centres of mass.

5.1. $\alpha \neq 0$

When two (or more) clusters of differently oriented Burgers vectors join due to the mutual attraction, two different configurations may be created. In the first one, each cluster keeps its own orientation and, therefore, the complex formed becomes immobile. This configuration may be metastable depending on the temperature and size of clusters and it can be transformed into the second one.

To form the second configuration the crowdions belonging to one cluster *individually* reorient themselves to the orientation of the other cluster, i.e., one cluster changes its Burgers vector to be parallel to the other, so that a bigger glissile and mobile cluster is formed. The mechanism shown is a favourable way for clusters to change their orientation and, therefore, the direction of their otherwise one-dimensional glide.

In this type of reaction we can directly observe the difference in behaviour of clusters and dislocation loops since the reaction does not follow the rule of summation of Burgers vectors. So, when the defect is big enough to behave as a proper dislocation loop it cannot follow such mechanism of reorientation. This is the case of the big clusters studied which have kept their initial Burgers vector. Therefore, such clusters (e.g., 37–61 SIAs) in both Cu and Fe behave like dislocation loops.

Of course, the mechanism of interaction (i.e., cluster-like or dislocation loop-like) depends on temperature and other parameters of the reaction meaning that the definition of big cluster or small dislocation loop is still qualitative and depends on the particular situation. For example, this is the case of two clusters in Cu at $\alpha = 90°$ which were not reoriented.

Note that the immobile complexes formed by non-transformed clusters can grow further due to the interaction with SIAs and other SIA clusters. Similar configurations have been observed in irradiated Cu [27].

Summarising, a glissile cluster can change, under certain conditions, its Burgers vector and gliding direction by reorienting its interstitials one by one from one crowdion orientation to another. This is a low energy process that occur during the interaction with another cluster. This mechanism does not follow the summation law of Burgers vectors and therefore allows to discriminate between clusters and dislocation loops.

5.2. $\alpha = 0$

Although the distortion of the lattice produced by a cluster is only along the crowdion direction [12,15], two non-overlapping clusters of parallel Burgers vector separated by several rows of atoms can interact effectively. This interaction is always attractive for Fe but can be repulsive for Cu clusters depending on the temperature and the initial separation between them. Since this interaction is repulsive at large distances, one can expect a much smaller probability of creation of such complexes in Cu.

In the simulation, using periodic boundary conditions, one cluster is always interacting either with the other cluster or its image, therefore when two clusters suffer repulsion they are forced to keep a fixed distance and, at high enough temperature, they can overcome the repulsive barrier as it occurs in Cu. Although the latter situation cannot be applied directly to freely gliding clusters, nevertheless, this result demonstrates that, under certain conditions, when the repulsion can be overcome (e.g., due to the interaction with other clusters and defects) stable complex of SIA clusters in copper can also be formed.

An interesting result is the qualitative difference in properties of such complexes created in Fe and Cu. Thus, a complex of two 19-SIA clusters in Fe is still mobile and produces atomic displacements whereas the equivalent complex in Cu is immobile. This is clearly demonstrated in Fig. 10 where the sum of the square displacements of atoms onto the glide direction is presented for both complexes in Fe and Cu at low temperature.

Since two 19-SIA clusters in Fe form a 38 SIA complex which is mobile we have compared this complex with the regular compact cluster of 37 interstitials. We found that their properties are different. The main difference is in the correlation of jumps of their common CM. We suppose that bigger complexes, e.g., having more clusters, can be immobile in Fe due to the decreasing of the value of the effective correlation factor below unity. Once such a complex is created it has a bigger cross-section to catch other SIA clusters than a compact cluster of the same number of interstitials. Since there is no repulsion between Fe clusters, we can

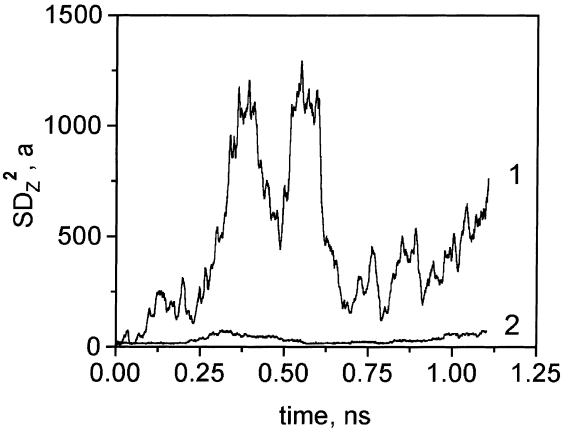

Fig. 10. Sum of the square of atomic displacements projected onto glide direction during thermal annealing of two joined 19-SIAs clusters (1) Fe at 260 K and (2) Cu at 310 K.

admit that such complexes can be formed and grown in bcc metals under irradiation. We suggest that this mechanism can be one of the possible explanations of the formation of rafts of dislocation loops observed experimentally in some bcc metals [28–30].

5.3. Qualitative differences between the interactions in Fe and Cu

The results presented here show qualitative differences in the interactions between interstitial clusters and loops in Fe and Cu. The main difference is that in Fe almost all types of the attractive interactions studied lead to the formation of a mobile cluster of bigger size. On the contrary, in Cu there is a probability to form immobile and even sessile clusters. Moreover, the critical size for a cluster to become loop is bigger in Fe than in Cu. These differences in the behaviour of SIA clusters and loops in Fe and Cu can contribute to the understanding of the difference in the radiation damage in Fe and Cu and, in general, in bcc and fcc metals.

Acknowledgements

This research has been carried out using the facilities of CESCA and CEPBA (Barcelona, Spain) under the coordination of C4 and under the project PB96-0170-CO3-03 from DGES. Yu.N.O. acknowledges the Research Fellowship from the University of Liverpool.

References

[1] C.H. Woo, B.N. Singh, Phys. Stat. Sol. B 159 (1990) 609.
[2] C.H. Woo, B.N. Singh, Philos. Mag. A 65 (1992) 889.
[3] B.N. Singh, A.J.E. Foreman, Philos. Mag. A 66 (1992) 975.
[4] H. Trinkaus, B.N. Sing, A.J.E. Foreman, J. Nucl. Mater. 206 (1993) 200.
[5] B.N. Sing, S.I. Golubov, H. Trinkaus, A. Serra, Y.N. Osetsky, A.V. Barashev, J. Nucl. Mater. 251 (1997) 107.
[6] B.D. Wirth, G.R. Odette, D. Maroudas, G.E. Lucas, J. Nucl. Mater. 244 (1997) 185.
[7] Y.N. Osetsky, A. Serra, V. Priego, Mater. Res. Soc. Symp. 527 (1998) 59.
[8] N. Soneda, T. Diaz de la Rubia, Philos. Mag. A 78 (1998) 995.
[9] Y.N. Osetsky, D.J. Bacon, A. Serra, Mater. Res. Soc. Symp. 540 (1999) 649.
[10] Y.N. Osetsky, V. Priego, A. Serra, B.N. Singh, S.I. Golubov, Philos. Mag. A (in press).
[11] Y.N. Osetsky, A. Serra, B.N. Singh, S.I. Golubov, Philos. Mag. A (submitted).
[12] Y.N. Osetsky, D.J. Bacon, A. Serra, B.N. Singh, S.I. Golubov, these Proceedings, p. 65.
[13] A.V. Barashev, Y.N. Osetsky, D.J. Bacon, Mater. Res. Soc. Symp 540 (1999) 697.
[14] A.V. Barashev, Y.N. Osetsky, D.J. Bacon, Philos. Mag. A (submitted).
[15] Y.N. Osetsky, D.J. Bacon, A. Serra, Philos. Mag. Lett. 79 (1999) 273.
[16] D.J. Bacon, F. Gao, Y.N. Osetsky, Proc. COSIRES-98 Nucl. Instrum. and Meth. B 153 (1999) 87.
[17] D.J. Bacon, F. Gao, Yu.N. Osetsky, these Proceedings, p. 1.
[18] F. Gao, Yu.N. Osetsky, D.J. Bacon, P.E.J. Flewitt, T.A. Lewis, these Proceedings, p. 213.
[19] B.N. Sing, A.J.E. Foreman, H. Trinkaus, J. Nucl. Mater. 249 (1997) 103.
[20] R. Bullough, R.C. Perrin, Proc. Roy. Soc. A 305 (1968) 541.
[21] E. Kuramoto, these Proceedings, p. 143.
[22] Y.N. Osetsky, A.G. Mikhin, A. Serra, Philos. Mag. A 72 (1995) 361.
[23] Y.N. Osetsky, M. Victoria, A. Serra, S.I. Golubov, V. Priego, J. Nucl. Mater. 251 (1997) 34.
[24] Y.N. Osetsky, A. Serra, M. Victoria, S.I. Golubov, V. Priego, Philos. Mag. A (in press).
[25] E.A. Little, B.L. Eyre, J. Microsc. 97 (1973) 107.
[26] E.A. Little, B.L. Eyre, Met. Sci. 7 (1973) 100.
[27] E.A. Little, R. Bullough, M.H. Wood, Proc. Roy. Soc. A 372 (1980) 565.
[28] R. Bullough, in: M.H. Loretto (Ed.), Dislocations and Properties of Real Materials, The Institute of Metals, London, 1985, p. 283.
[29] J.L. Brimhall, B. Mastel, Radiat. Eff. 3 (1970) 203.
[30] B.N. Sing, J.H. Evans, A. Horsewell, P. Toft, G.V. Müller, J. Nucl. Mater. 258–263 (1998) 865.